**Laboratory Investigation (2017) 97,** 1488–1499


# Expression, function, and regulation of the embryonic transcription factor TBX1 in parathyroid tumors

Chiara Verdelli[1], Laura Avagliano[2], Vito Guarnieri[3], Filomena Cetani[4], Stefano Ferrero[5,6], Leonardo Vicentini[7], Edoardo Beretta[8], Alfredo Scillitani[9], Pasquale Creo[10], Gaetano Pietro Bulfamante[2], Valentina Vaira[5,11] and Sabrina Corbetta[12]

Transcription factors active in embryonic parathyroid cells can be maintained in adult parathyroids and be involved in tumorigenesis. *TBX1*, the candidate gene of 22q11.2-DiGeorge syndrome, which includes congenital hypoparathyroidism, is involved in parathyroid embryogenesis. The study aimed to investigate expression, function, and regulation of the parathyroid embryonic transcription factor TBX1 in human parathyroid adult normal and tumor tissues. *TBX1* transcripts were detected in normal parathyroids and were deregulated in parathyroid tumors. Using immunohistochemistry, TBX1 protein was detected, mainly at the nuclear level, in a consistent proportion of cells in normal adult parathyroids, whereas TBX1 immunoreactivity was absent in fetal parathyroids. TBX1-expressing cells were markedly reduced in about a half of adenomas (PAds) and two-thirds of carcinomas and the proportion of TBX1-expressing cells negatively correlated with the serum albumin-corrected calcium levels in the analyzed tumors. Moreover, a subset of TBX1-expressing tumor cells coexpressed PTH. TBX1 silencing in HEK293 cells, expressing endogenous TBX1, increased the proportion of cells in the G0/G1 phase of cell cycle; concomitantly, *CDKN1A*/p21 and *CDKN2A*/p16 transcripts increased and *ID1* mRNA levels decreased. *TBX1* silencing exerted similar effects in PAd-derived cells, suggesting cell cycle arrest. Moreover, in PAd-derived cells *GCM2* and *PTH* mRNA levels were unaffected by TBX1 deficiency, whereas it was associated with reduction of *WNT5A*, an antagonist of canonical WNT/β-catenin pathway. WNT/β-catenin activation by lithium chloride inhibited *TBX1* expression levels both in HEK293 and PAd-derived cells. In conclusion, TBX1 is expressed in adult parathyroid cells and deregulated in parathyroid tumors, where TBX1 deficiency may potentially contribute to the low proliferative nature of parathyroid tumors.
*Laboratory Investigation* (2017) **97,** 1488–1499; doi:10.1038/labinvest.2017.88; published online 18 September 2017

The role of embryonic development determinants in human tumorigenesis is an emergent evidence for parathyroid tumors. Nuclear transcription factors involved in parathyroid embryogenesis such as glial cells missing homolog 2 (GCM2),[1] homeobox A3 (HOXA3),[2] and GATA3 (refs 3,4) have been found to be expressed in human adult parathyroid tissues. *GCM2* gene inactivation determines congenital isolated hypoparathyroidism,[5–7] and deregulation of its expression has been observed in parathyroid adenomas (PAds) compared with normal glands, although with opposite readouts.[8,9] Moreover, developmental *HOX* group 3 gene paralogs are deregulated in human *MEN1*-related and sporadic parathyroid tumors compared with normal glands.[10] Again, the embryonic microRNA clusters C19MC and miR-371-373 on chromosome 19 are aberrantly expressed in a consistent subset of parathyroid tumors.[11]

The T-box transcription factor TBX1, the candidate gene for the 22q11.2 microdeletion/DiGeorge syndrome,[12] has emerged as a central factor in the coordinated formation of organs and tissues derived from the pharyngeal pouches.[13] DiGeorge syndrome spans over a wide range of phenotypes, involving heart conotruncal defects, deafness, mental

[1]Laboratory of Experimental Endocrinology, IRCCS Istituto Ortopedico Galeazzi, Milan, Italy; [2]Unit of Human Pathology, Department of Health Sciences, San Paolo Hospital Medical School, University of Milan, Milan, Italy; [3]Department of Medical Genetics, IRCCS Hospital Casa Sollievo della Sofferenza, San Giovanni Rotondo (FG), Italy; [4]Endocrine Unit 2, University Hospital of Pisa, Pisa, Italy; [5]Division of Pathology, Fondazione IRCCS Cà Granda Ospedale Maggiore Policlinico, Milan, Italy; [6]Department of Biomedical, Surgical and Dental Sciences, University of Milan, Milan, Italy; [7]Endocrine Surgery, IRCCS Fondazione Cà Granda Ospedale Maggiore Policlinico, Milan, Italy; [8]Endocrine Surgery, IRCCS Ospedale San Raffaele, Milan, Italy; [9]Endocrine Unit, IRCCS Hospital Casa Sollievo della Sofferenza, San Giovanni Rotondo (FG), Italy; [10]Laboratory of Stem Cells for Tissue Engineering, IRCCS Policlinico San Donato, Milan, Italy; [11]Department of Clinical/Surgical Pathophysiology and Organ Transplantation, University of Milan, Milan, Italy and [12]Department of Biomedical Sciences for Health, Endocrinology Service, Laboratory of Experimental Endocrinology, University of Milan, IRCCS Istituto Ortopedico Galeazzi, Milan, Italy
Correspondence: Professor S Corbetta, MD, PhD, Department of Biomedical Sciences for Health, Endocrinology Service, Laboratory of Experimental Endocrinology, University of Milan, IRCCS Istituto Ortopedico Galeazzi, Via R.Galeazzi 4, 20161 Milan, Italy.
E-mail: sabrina.corbetta@unimi.it

Received 8 October 2016; revised 16 July 2017; accepted 19 July 2017

**Table 1 Genetic and clinical features of the investigated parathyroid carcinomas**

| No. | Sex | Age, years | LOH 1q25 | CDC73 mutations | G/S | Para | TBX1% cells | SCa mg/dl | PTH pg/ml | Met |
|---|---|---|---|---|---|---|---|---|---|---|
| 1[a] | F | 37 | No | c.518_521delTGTC | G | – | 5 | 13.0 | 660 | No |
| 2[a] | F | 55 | No | c.415C>T | G | – | 1 | 16.1 | 293 | Yes |
| 3[a] | F | 54 | No | c.679_680delAG | S | – | 1 | 17.6 | 940 | Yes |
| 4[a] | F | 26 | No | c.679_680delAG | G | – | 10 | 11.5 | 106 | No |
| 5 | F | 37 | Yes | No | — | + | 45 | 11.2 | 845 | No |
| 6 | F | 57 | Yes | c.679_680delAG | G | – | 0 | 15.0 | 320 | No |
| 7 | F | 70 | Yes | c.679_680delAG | S | – | 5 | 11.6 | 563 | No |
| 8 | M | 23 | No | c.94insTA | S | – | 15 | 16.5 | 353 | No |
| 9 | F | 47 | No | No | — | + | 45 | 11.7 | 642 | No |
| 10 | M | 54 | No | No | — | + | 60 | 12.0 | 253 | No |
| 11 | F | 44 | No | No | — | + | 50 | 13.7 | 1347 | No |
| 12 | M | 57 | No | No | — | + | 50 | 14.9 | 690 | No |
| 13 | M | 45 | Yes | R234X | S | – | 0 | 16.0 | 1850 | Yes |
| 14 | F | 32 | No | R234X | S | – | 1 | 15.5 | 720 | Yes |

+, positive immunostaining for parafibromin (>10% of cells); −, negative immunostaining for parafibromin; CDC73, cell cycle division 73; G, germline; LOH, loss of heterozygosity; Met, metastasis; Para, immunohistochemistry on FFPE sections for parafibromin; S, somatic; SCa, serum albumin-corrected calcium; TBX1% cells, % of cells expressing TBX1 by immunohistochemistry.
[a]Previously reported cases.[23]

retardation, facial dysmorphisms, thymic immunity impairment, hypoparathyroidism, and hypothyroidism.[14,15] *Tbx1* ablation disrupts parathyroid embryonic development in mice: conditional endoderm null embryos at E17.5 lack parathyroid glands, whereas in *Tbx1* conditional heterozygous embryos, parathyroid glands are ectopically placed,[16] suggesting that parathyroid cells are sensitive to the *Tbx1* gene dosage.

During embryogenesis, TBX1 supports cell proliferation and inhibits cell differentiation. Recently, experimental data suggest an involvement in the mechanisms of cell morphology, cell dynamics, and cell–cell interactions and adhesion.[17] TBX1 is neither a strong transcriptional activator nor a strong repressor, although it regulates a large number of genes through epigenetic modifications, interacting with histone modifiers and chromatin-remodeling complexes.[17] Members of the T-box transcription factors' family show in the adult life functions distinct to those driven during embryonic development, being also involved in tumorigenesis: TBX2, TBX3, and brachyury are expressed in a number of human neoplasia[18–20] and TBX1 has been involved in mouse and human skin tumor development[21] and in basal cell carcinomas.[22]

No data about the expression and the role of the *TBX1* gene in human adult parathyroid tissues are available so far. In the present study, we first investigated TBX1 expression, function, and regulation in human normal, adult, and fetal, and tumor parathyroid tissues providing data about deregulation of TBX1 in parathyroid tumors.

## MATERIALS AND METHODS

### Sample Collection

Formalin-fixed paraffin-embedded (FFPE) sections from five normal parathyroid glands (PaNs) accidentally removed during thyroid surgery from normocalcemic patients and 44 parathyroid tumors (30 PAds and 14 parathyroid carcinomas) from patient with primary hyperparathyroidism (PHPT) were collected. Clinical and biochemical features of PCas are reported in Table 1. PHPT patients (22 females and 8 males), aged 56.5 (52.7–63.5) years, harboring a single sporadic PAd, had median serum albumin-corrected calcium 11.3 (11.0–11.8) mg/dl, serum PTH 153 (108.8–370.8) pg/ml, and tumor weight 1.5 (1.4–2.1) g (median (range interquartile)). Parathyroid glands from fetuses of gestational ages 19 and 25 weeks were obtained as previously described.[23] In all cases, informed consent of the mother was obtained before procurement of the tissues.

Fetal and adult samples were formalin-fixed and paraffin-embedded following standard histological procedures. Four-micrometer-thick sections were cut and stained with hematoxylin and eosin for morphological assessment before immunohistochemistry. Histological diagnosis of parathyroid carcinoma was established according to the WHO published guidelines[24] and sampled as previously described.[25]

Fresh tissue samples from 30 parathyroid typical adenomas were collected for further investigations. Tissues removed were in part placed in a sterile medium for cell culture and in part snap-frozen in liquid nitrogen and stored at −80 °C until analysis. The study was approved by the local Ethical

Committee and informed consent was obtained from all patients.

### Immunohistochemistry

Both adult and fetal parathyroid tissue sections were incubated with a rabbit monoclonal primary antibody specific for TBX1 (1:400 dilution; Epitomics, AVIVA Systems Biology, San Diego, CA, USA). Parathyroid carcinoma sections were incubated with a mouse monoclonal antibody to human parafibromin (1:50 dilution; clone sc-33638, Santa Cruz Biotechnology, Dallas, TX, USA) as previously described.[26–28] TBX1 and parafibromin immunoreactivity could be evaluated in five PaNs, 13 PAds (seven stained for parafibromin), and in 14 carcinomas (PCas). Samples were considered IHC-negative for parafibromin if they did not reveal any nuclear staining at all.[27] Fetal parathyroid sections were analyzed with a mouse monoclonal antibody anti-podoplanin/D2-40 (1:200 dilution; D2-40, Dako) and a mouse monoclonal antibody anti-$\alpha$ smooth muscle actin ($\alpha$SMA; 1:200 dilution; ab5694, Abcam). Immunohistochemical staining was performed using the automatic staining BioGenex i6000 Automated Staining System (BioGenex, Fremont, CA, USA). Reactions were detected by Novolink Polymer Detection System (Novocastra Laboratories, Leica Microsystems), according to the manufacturer's instructions. Negative controls were incubated in the absence of primary antibody, and a positive control core (referee) was used to standardize immunoreactivity between slides. For TBX1 evaluation, the percentage of positive nuclei was scored out of the total number of parathyroid cells present in four high-power fields. Accordingly, at least 500 cells per sample were counted as previously described for other markers.[29] Scoring and interpretation of immunohistochemical results were performed by two pathologists (SF and VV) and a consensus was reached for all cases.

### DNA Extraction and CDC73/HRPT2 Gene Sequencing

Genomic DNA was purified from the peripheral blood and tumor specimens from patients affected with PCas using the phenol–chloroform protocol. The entire coding region and splice site junctions of the *CDC73/HRPT2* gene were PCR-amplified and directly sequenced as previously described.[28,30,31] Data were presented in Table 1.

### RNA Extraction, RT-PCR, and Taqman Real-Time PCR

Total RNA from fresh collected and cryopreserved samples of human adult normal kidney, liver, and parathyroid gland were purified with TRIzol reagent (Gibco-Invitrogen, Life Technologies, Carlsbad, CA, USA) according to the manufacturer's instruction and were retrotranscribed to cDNA using random hexamers and the High Capacity cDNA Transcription kit (Life Technologies). In order to avoid any amplification from genomic DNA contamination, RNA samples were all pretreated with DNase. Reverse-transcribed RNA was analyzed for *TBX1* gene expression by PCR amplification using specific primers (sequence available upon request). The housekeeping *ACTB* gene was used as internal control. Amplified RT-PCR products were then analyzed on 1.5% agarose gels and visualized using ethidium bromide staining and a camera system (CHEMI DOC XRS, Bio-Rad) and were compared with a DNA Molecular Weight Marker (Roche). The specific bands were isolated and sequenced to assure that they represented the expected products, using an automated sequencer (PerkinElmer, Norwalk, CT).

Total RNA from 30 PAd, 14 PCa, and 5 PaN FFPE specimens was purified with TRIzol reagent (Gibco-Invitrogen, Life Technologies) according to the manufacturer's instruction and was retrotranscribed to cDNA using random hexamers and the High Capacity cDNA Transcription kit (Life Technologies). RNA quality obtained from FFPE section was tested by amplification of housekeeping genes. Amplification of the *TBX1* gene in the FFPE series provides results similar to those obtained from cryopreserved corresponding tumor samples ($n = 10$) showing a good correlation. Real-Time PCR was conducted on an ABI PRISM 7900HT Sequence Detection System (Life Technologies) using pre-configured Taqman gene expression assay for target genes (*TBX1* Hs00271949_m1; *WNT5A* Hs00998537_m1; *SMAD7* Hs00998193_m1; *ID1* Hs00357821_g1; *CDKN1A*/p21 Hs00355782_m1; *CDKN2A*/p16 Hs00923894_m1; *PTH* Hs00757710_g1; *GCM2* Hs00899403_m1 Applied Biosystems), or reference genes (HMBS Hs00609297_m1, b2M Hs99999907_m1), as previously described.[25] Instruments' raw data were converted into Ct values by SDS 2.1 software and target gene expression was relatively quantified on internal controls (HMBS and b2M) using the comparative Ct method. All experiments were repeated for at least three times to ensure the accuracy of results.

### Culture of PAd-Derived Cells and HEK293 Cells

Fresh-collected samples from PAds were cut into fragments less than 1 $mm^3$, washed with PBS, and partially digested with 2 mg/ml collagenase type I (Worthington, Lakewood, NJ, USA). After digestion, tissue fragments were filtered with a cell strainer (100 $\mu$m Nylon, BD Falcon). Both human PAd-derived and HEK293 cells were routinely grown at 37 °C, 5% $CO_2$ in Dulbecco's modified Eagle's medium supplemented with 10% fetal bovine serum, 2 mmol/l glutamine, and 100 U/ml penicillin–streptomycin.

### Protein Extraction and Western Blot Analysis

PAd whole tissues and dispersed PAd-derived single cells were homogenized using a Nuclear Extract kit (Active Mitif, Carlsbad, CA, USA) following the manufacturer's instructions in order to obtain both cytoplasmic and nuclear protein fractions. After separation by SDS-PAGE, polypeptides were electrophoretically transferred to nitrocellulose membrane (Bio-Rad, USA), and antigens were revealed by respective primary antibodies (TBX1 and Calnexin, Epitomics; MYC, p21, phospho-$\beta$-catenin (Ser33/37/Thr41) and total $\beta$-catenin, Cell Signaling, Danvers, MA, USA; GAPDH MAB374,

Millipore, Billerica, MA, USA) and the appropriate secondary HRP-conjugated goat anti-rabbit or anti-mouse antibodies (Goat anti-rabbit IgG (H+L) HRP, 3053-1 Epitomics; Goat anti-mouse IgG HRP-linked, 7076 Cell Signaling). Calnexin or GAPDH was used as internal controls. Proteins were visualized by ECL (Thermo Scientific, USA) and quantified by densitometric readings (Image-J).

The rabbit monoclonal anti-human TBX1 antibody by Epitomics was raised against an epitope within the amino acids 90–120 of the human TBX1; it recognized a band of ~53 kDa in HEK293 and Caco-2 cell extracts, used as positive controls, corresponding to the TBX1 isoform C. Both in HEK293 and PAd-derived cells, specific bands were detected in the cytoplasmic and nuclear fractions. The specificity of the antibody was confirmed by experiments with TBX1 short interfering RNA (siRNA) both in HEK293 and in PAd-derived cells, where the bands of 53 kDa were definitely reduced. Immunohistochemistry and immunofluorescence were performed with the same anti-TBX1 antibody, which, in agreement with western blot results, detected TBX1 at cytoplasm and nuclear levels.

### Immunofluorescence

PAd-derived cells were fixed in 4% paraformaldehyde, permeabilized in 0.2% Triton X-100, and blocked in free serum-free block protein solution (DAKO) for 1 h. Cells were incubated with primary antibodies, TBX1 (Epitomics and Santa Cruz Biotechnology), and PTH (Santa Cruz Biotechnology), washed three times in PBS, and then incubated with secondary antibodies conjugated with Alexa488 or Cy3 (Jackson Immuno Research; 1:100). Hoechst 33342 was used as the nuclear stain (blue). As negative control, PBS was used instead of primary antibodies to exclude unspecific binding of secondary antibody. Images were obtained using confocal microscopy (Zeiss LSM 510 System, Oberkochem, Germany) for PAd-derived cells and fluorescence microscopy (Zeiss Axioskop 2 Plus) for HEK293 cells.

### TBX1 Gene Silencing

Short hairpin RNA (shRNA) Lentiviral Particles (Santa Cruz Biotechnology), which encode 19–25 nucleotide shRNA, were used to knockdown TBX1 protein expression in HEK293 cells. The infection at MOI of 10 was performed using TBX1 shRNA Lentiviral Particles (sc-38467-V), which are a pool of transduction-ready viral particles containing three target-specific constructs that encode shRNA designed to knock-down TBX1 expression, and Control shRNA Lentiviral Particles (sc-108080), which represent the negative control of the transfection experiments because those particles encode a scrambled shRNA sequence that does not lead to the specific degradation of any known cellular mRNA. After infection, cells stably expressing TBX1 shRNA or Control were isolated by puromycin selection (5 $\mu$g/ml). Puromycin-resistant cells with stable silencing of TBX1 were cultured in complete medium and were used for gene expression and cell cycle analysis.

PAd-derived cells were not suitable for stable transfection because of their low proliferative rate; therefore, specific TBX1 siRNA (siGENOME Smart pool, Dharmacon) was used following the manufacturer's instructions. Briefly, a total of $5 \times 10^5$ cells were plated in six-well plates and transfected using 100 pmol siRNA and 5 $\mu$l of Lipofectamine 2000 (Life Technologies) per well. After 6 h of incubation, 2 ml of fresh growth medium was added to the cells. Following 48 h of incubation, the cells transiently transfected were harvested for analysis.

### Cell Cycle Analysis

Analysis of cell cycle progression was performed using propidium iodide (PI) staining. HEK293 cells were washed twice in PBS and fixed with cold 100% EtOH overnight at − 20 °C. Cells were washed twice in PBS and resuspended in 500 $\mu$l of a solution composed of PBS, 1% BSA, 0.5% Tween, 1 $\mu$l of RNAse, and 10 $\mu$l of PI solution (BioLegend, San Diego, CA, USA) and were incubated for 15 min at 4 °C. Cells were analyzed by flow cytometry (Navios, Beckman Coulter, Milan, Italy) using Kaluza Software.

### Statistics

Data are expressed as mean ± s.e.m. When comparing the data from two series, paired two-tailed Student's *t*-test, Mann–Whitney *U*-test, or one-way analysis of variance were used as appropriate to determine levels of significance. Categorical data were analyzed by $\chi^2$-or Fischer exact test, as appropriate. Correlations between two variables were analyzed by linear regression analysis or Spearman test as appropriate. A *P*-value of $<0.05$ was considered statistically significant.

## RESULTS

### Expression of the Embryonic Transcription Factor TBX1 in Human Parathyroid Tissues

*TBX1* transcripts could be detected using RT-PCR with specific primers in the total RNA from human adult normal kidney, used as positive control, and in human adult PaN (Figure 1A); the liver was used as negative control. Quantification of *TBX1* transcripts with real-time PCR, using a specific probe directed against the sequence codifying the common portion of the three known *TBX1* isoforms, showed that the *TBX1* gene was variably deregulated in parathyroid tumors compared with PaNs. In particular, considering as significant a variation of *TBX1* mRNA levels greater than two folds the mean levels dected in five PaNS, *TBX1* gene expression was deregulated in 12 (40%) out of 30 PAds and in 10 (71%) out of 14 PCas (Figure 1B). All PCa samples and a subset of PAds (5 out of 12) had reduced *TBX1* expression levels, whereas in seven PAd samples *TBX1* mRNA levels were higher than the mean levels in normal glands (Figure 1B). TBX1 protein expression in adult parathyroid tissues was

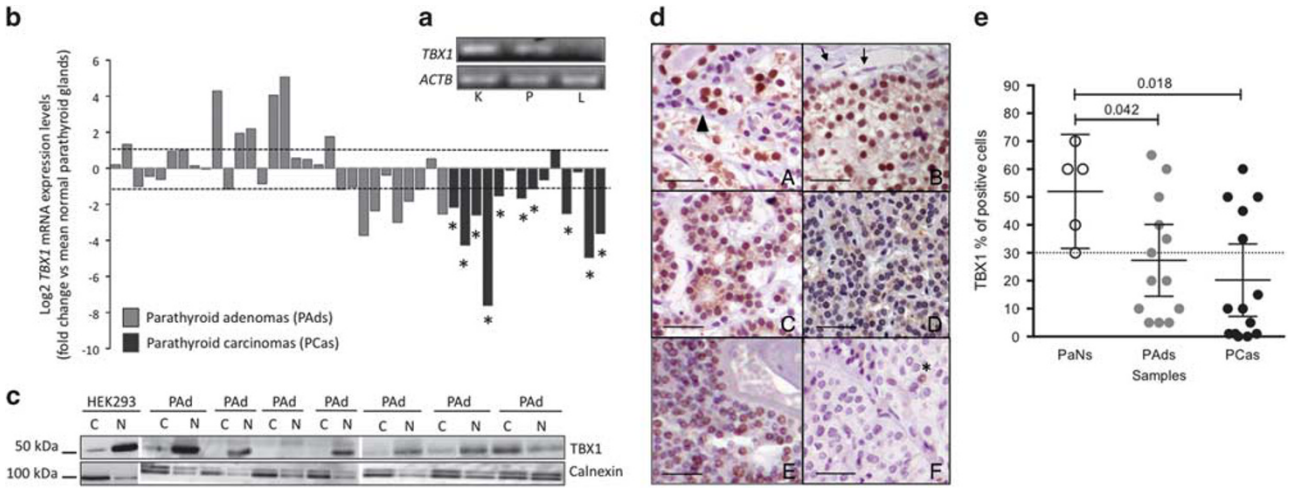


**Figure 1** TBX1 transcripts and proteins in human parathyroid tissues. (**a**) RT-PCR amplification products of the *TBX1* gene in human adult normal kidney (K), parathyroid (P), and liver (L) samples. (**b**) Quantitative real-time PCR analysis of the *TBX1* gene expression in RNA samples from 30 parathyroid adenomas (PAds) and 14 parathyroid carcinomas (PCas). *TBX1* mRNA expression levels were represented as log2 of fold changes with respect to the mean of the *TBX1* mRNA levels in five normal glands. Dash lines indicate ± 2-folds the mean of normal parathyroid levels: expression levels below or above these limits were considered as significantly deregulated. *, PCa samples with negative parafibromin immunostaining. (**c**) Representative immunoblot by monoclonal anti-TBX1 antibody of fractioned proteins (C, cytoplasmic; N, nuclear) from seven PAds identifying the TBX1 isoform C of 53 kDa. (**d**) Representative images of the TBX1 immunostaining in normal parathyroids (A, B); arrows, TBX1-negative endothelial cells; arrowheads, TBX1-negative fibroblasts; C, E show a PAd (C) and a parathyroid carcinoma (E) with a proportion of TBX1-expressing cells similar to that in normal glands; D, F show a PAd (D) and a parathyroid carcinoma (F) with definitely reduced TBX1-expressing cells. *, a scattered TBX1-expressing cell. All sections were imaged at ×40 magnification. Scale bars, 100 μM. (**e**) Quantification of TBX1-positive parathyroid cells in the indicated tissue types. Seven PAd and eight PCa samples showed that a proportion of TBX1-expressing cells definitely reduced compared with normal glands (PaNs; <30%). *P*-values are from Mann–Whitney *U*-test.

investigated by western blot analysis on the cytoplasm and nuclear-fractioned proteins from PAd samples ($n = 11$) and by immunohistochemistry on FFPE sections from 13 PAds and 14 PCas by a specific monoclonal anti-human TBX1 antibody. Immunoblotting identified in all samples a band of ~53 kDa, likely corresponding to the isoform C of 495 aa, mainly expressed in the nuclear fractions (Figure 1C), characterized by a great variability.

Immunohistochemistry on FFPE sections showed specific nuclear expression of TBX1 protein detectable in all normal glands from normocalcemic patients ($n = 5$; Figure 1Da and b and Supplementary Material) with variable levels, ranging from 30 to 70% of parathyroid cells (mean ± s.e.m., 52.0 ± 7.3%), where it was occasionally associated with cytoplasm staining for TBX1 (Figure 1Da). Endothelial and stromal cells within the parathyroids were TBX1-negative (Figure 1Dd). Opposite to what observed in non-pathological condition, PAds from patients with PHPT ($n = 13$) showed reduction in nuclear expression of TBX1 (Figure 1Dc and d), with seven cases (54%) displaying less than 30% of positive cells (lowest percentage detected in normal samples; range: 5–65%; mean: 27.3%; Figure 1Dd and E). More interestingly, 9 PCas out of 14 (64%) showed a decrease in the percentage of TBX1-positive cells relative to normal samples (range 0–60%; mean 20.2%; Figure 1De, f and E). The decrease in TBX1-positive cells measured in PAds or PCas compared with that in controls was statistically significant ($P = 0.042$ and 0.018 by Mann–Whitney *U*-test; Figure 1E). From a histological point of view, in parathyroid tumors with a reduced number of TBX1-expressing cells (ie, less than 30%), TBX1-positive cells were found as single interspersed entities in the tumor parenchyma (Figure 1Df and Supplementary Materials).

Comparing the *TBX1* mRNA and protein expression profiles, discrepancies emerged: in PAds, both upregulation and downregulation of *TBX1* transcripts were associated with loss of TBX1-expressing cells in a half of tumor samples, whereas PCas showed concordant reduction of *TBX1* transcript levels and loss of TBX1-expressing cells (Figure 2A). These data may suggest that a specific *TBX1* gene dosage is required for TBX1 protein generation in parathyroid tumor cells.

Immunofluorescence showed that a subset of TBX1-expressing cells derived from PAds coexpressed PTH (Figure 2B), indicating that TBX1 is also expressed in hormonally active parathyroid cells. Therefore, potential correlation with biochemical parameters was investigated: any significant correlation could be detected between the proportion of TBX1-expressing cells and serum PTH levels or tumor weights, whereas serum albumin-corrected calcium levels negatively correlated with the proportions of TBX1-positive cells (Figure 2C), suggesting an association between the loss of TBX1-expressing cells and the biochemical severity of the primary hyperparathyroidism.

We also correlated TBX1 expression with one of the most studied oncosuppressor gene in parathyroid neoplasia, parafibromin. Parafibromin is the product of the

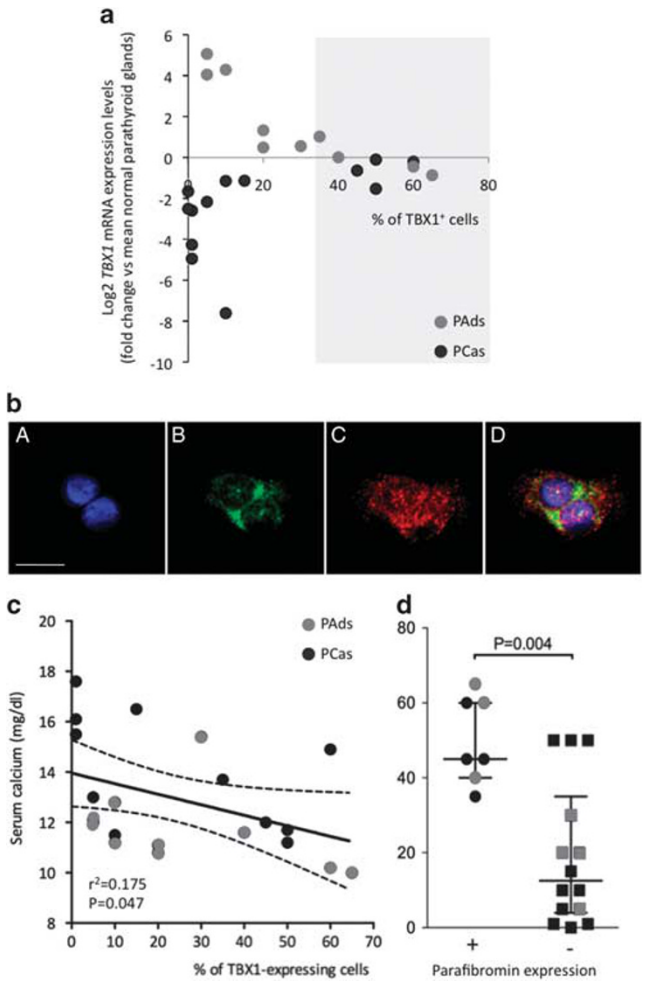


**Figure 2** Correlation between TBX1 expression and biochemical markers in human parathyroid tumors. (**a**) Correlation between *TBX1* mRNA levels and the proportion of TBX1-expressing cells detected by IHC; black circles, parathyroid carcinomas (PCas); grey circles, parathyroid adenomas (PAds); light grey area, percentages of TBX1-expressing ($TBX1^+$) cells in normal parathyroid glands. (**b**) Immunofluorescence analysis by monoclonal anti-TBX1 antibodies (red, C) in PAd-derived cells showing that TBX1-expressing cells coexpress PTH (green, B; merge, D); (A) nuclear DAPI staining. Sections were imaged with a confocal microscope at ×40 magnification. Scale bars, 100 μm. (**c**) Relationship between the proportions of TBX1-expressing cells and serum albumin-corrected calcium in patients harboring the analyzed tumors at diagnosis: serum calcium levels are inversely correlated with the proportion of TBX1-expressing levels; grey circles, PAds; black circles, PCas; dash lines, 95% confidence interval of linear regression analysis ($r^2 = 0.175$; $P = 0.047$). (**d**) Relationship between parafibromin and TBX1 expression: parathyroid tumors negative for nuclear parafibromin immunostaining (squares) have a median proportion of TBX1-expressing cells significantly lower than tumors expressing parafibromin (circles); grey symbols, PAds; black symbols, parathyroid carcinomas; bars represent medians and range interquartiles.

oncosuppressor gene *CDC73/HRPT2*, lost in most parathyroid carcinomas. The parafibromin expression pattern was determined in the present PCa series (Table 1) and correlated with TBX1 gene expression. Interestingly, the four carcinomas conserving parafibromin expression had *TBX1* mRNA expression levels similar to those of normal glands (Figure 1B) and a number of TBX1-expressing cells similar to those of normal glands at IHC (Table 1 and Figure 2D). By contrast, parafibromin-negative PCas showed variably reduced *TBX1* mRNA levels (Figure 1B) and most had a number of TBX1-expressing cells significantly lower than 30%, the lower limit of the range in normal glands (Table 1 and Figure 2D).

Finally, we had the opportunity to analyze TBX1 expression by immunohistochemistry in human fetal tissues from second trimester of pregnancy (19 and 25 weeks of gestational ages). Specific immunostaining for TBX1 was detected in the cytoplasm and nucleus of the αSMA-positive cells of stomach muscle layer and similarly in the skeletal muscle cells of ileopsoas (Supplementary Figure 1). TBX1 was expressed in the basal layer of tracheal epithelia and in endothelial cells of vessels. TBX1-expressing cells were also detected in fetal thyroid gland (Supplementary Figure 1c); indeed, location and expression of the podoplanin/D240 marker suggested that these cells lined lymphatic vessels. Although esophageal and parathyroid cells derive from the pharyngeal endoderm like tracheal epithelia, TBX1 immunostaining could not be detected in esophageal epithelial cells (Supplementary Figure 1g) as well as in abundantly expressing PTH parathyroid cells (Figure 3a, b and e). Indeed, TBX1 was faintly detectable in 19 weeks' fetal parathyroid glands (Figure 3b) and was definitely absent in parathyroid glands from 25 weeks of gestational age fetus (Figure 3f).

## Effects of TBX1 Gene Silencing in PAd-Derived Cells

### *Effects on cell cycle*

Because of the limited availability of PAd-derived cells, we were not able to investigate the effect of TBX1 silencing on cell cycle in these cells. HEK293 cells were used as an alternative model to parathyroid cells as they express the endogenous *TBX1* gene, both at mRNA and protein levels (Figure 4A). Stable silencing of the *TBX1* gene in HEK293 cells induced a significant reduction (~70%) of the nuclear TBX1 protein levels (Figure 4B). TBX1 deficiency increased the proportion of cells in the G0/G1 phase (from 43.3 ± 3.3 to 51.7 ± 8.7%, $P = 0.04$), suggesting that loss of TBX1 induces cell cycle arrest (Figure 4C and D).

### *Effects on gene targets*

Supporting the promotion of cell cycle arrest in HEK293 cells, TBX1 silencing increased *CDKN2A/p16* and *CDKN1A/p21* mRNA levels and decreased *ID1* mRNA levels (Figure 4E). Similar changes in the expression pattern of *CDKN2A/p16*, *CDKN1A/p21*, and *Inhibitor of differentiation 1 (ID1)* genes could be detected after 48 h of transient-efficient TBX1 silencing in PAd-derived cells (Figure 5A and B). The positive effect of TBX1 silencing on p21 protein levels could be detected in both HEK293 and PAd-derived cells (Figures 4E and 5A).

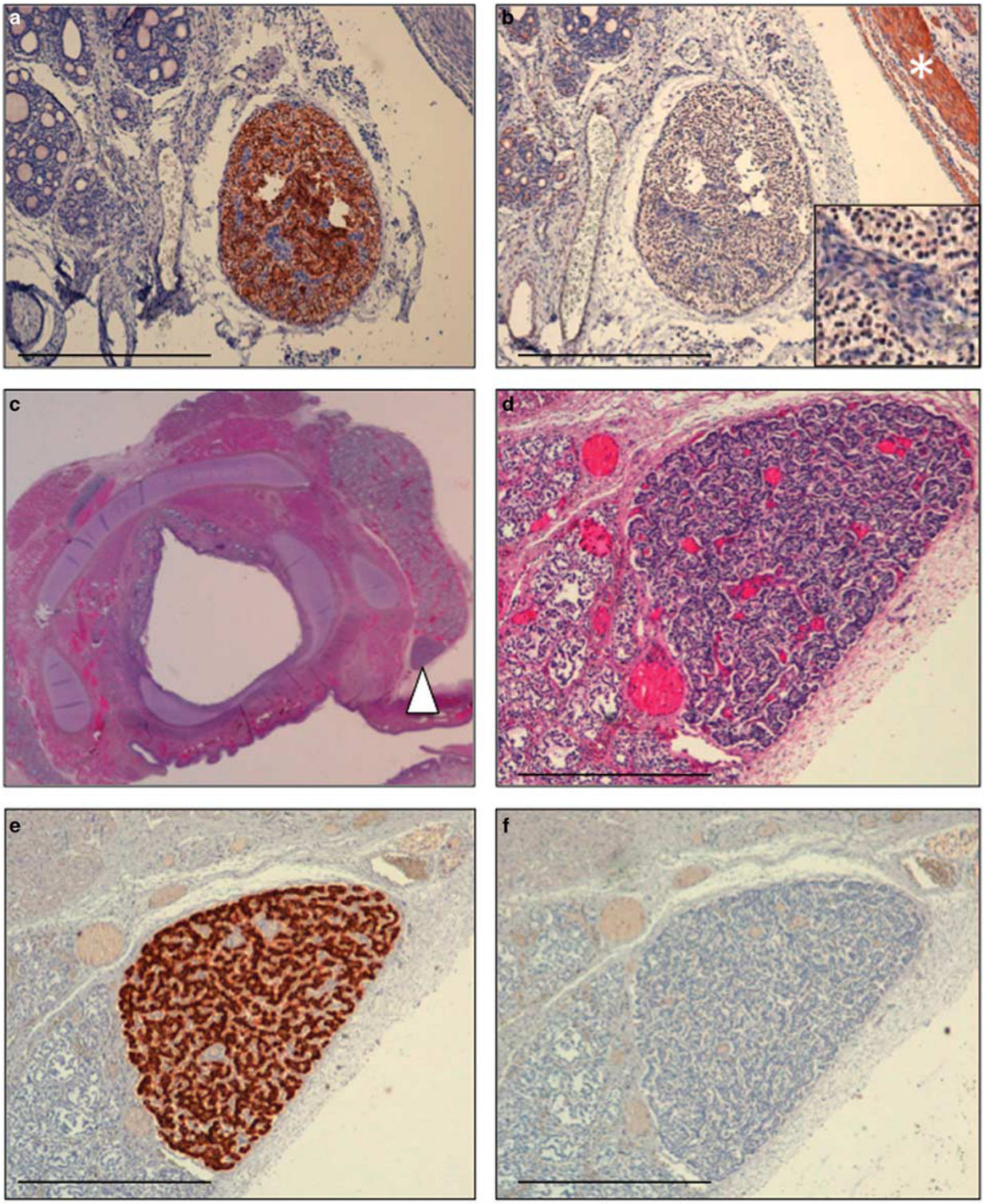


**Figure 3** TBX1 expression in human fetal parathyroid glands. Representative IHC by monoclonal anti-TBX1 antibodies of formalin-fixed paraffin-embedded (FFPE) samples of the pharyngeal region from 19 (**a**, **b**) and 25 (**c**–**f**) weeks of gestational-age fetuses. (**a**) Nineteen-week-fetal parathyroid gland showed homogenously positive PTH immunostaining; TBX1 immunostaining was faint (**b**; original magnification ×10; scale bar, 250 μm) and mainly nuclear (insert showing cells with TBX1-positive nuclei besides a cluster of cells with TBX1-negative nuclei; magnification ×40), whereas adjacent skeletal muscle was positive (*). Hematoxylin and eosin staining of the pharyngeal region from the 25-week-fetus showing a parathyroid gland posterior to thyroid gland (arrow head; **c**, **d**); original magnification of **d** image ×10; scale bar, 250 μm); the parathyroid gland showed a positive immunostaining for PTH (**e**); original magnification ×5; scale bar, 500 μm), whereas the staining for TBX1 was negative (**f**); original magnification ×5; scale bar, 500 μm).

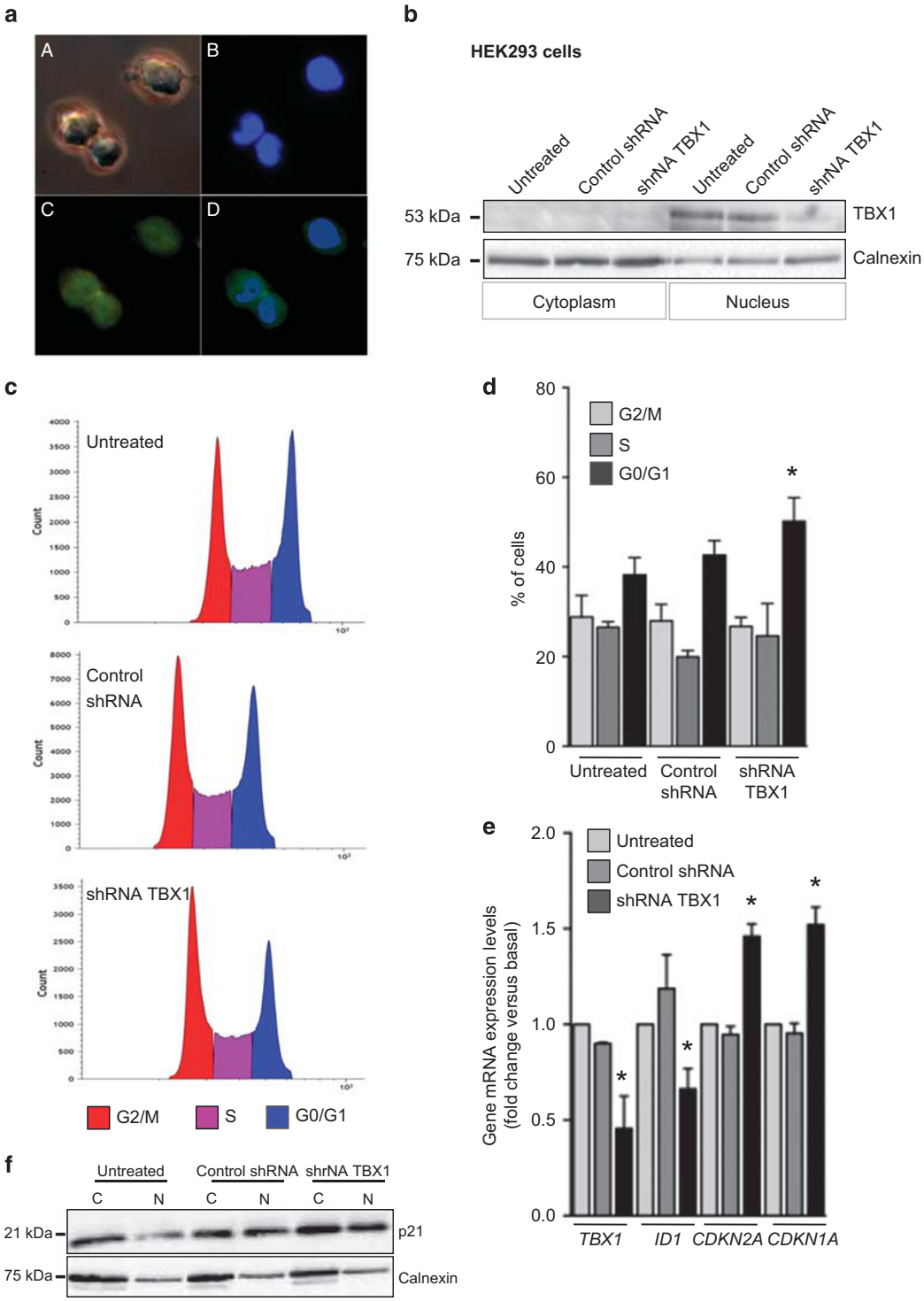


**Figure 4** Effects of TBX1 silencing in HEK293 cells. (**a**) Immunofluorescence showing that TBX1 is expressed in HEK293 cells at nuclear and cytoplasmic levels (green, C, D); (A) contrast phase correspondent image; (B) nuclei stained with DAPI (blue); (**b**) TBX1 protein is reduced in the nuclear fraction proteins by lentiviral stable silencing in HEK293 cells. (**c**) Representative cell cycle in TBX1-silenced HEK293 cells. (**d**) Effect of TBX1 silencing on proportions of HEK293 cells in different cell cycle phases; $^{*}P<0.05$ by ANOVA *vs* Control shRNA. (**e**) Effect of TBX1 silencing on the expression levels of genes involved in cell cycle regulation; $^{*}P<0.05$ by ANOVA *vs* Control shRNA for every analyzed gene. (**f**) Effect of TBX1 silencing on p21 protein levels.

Moreover, previously identified gene targets of TBX1, namely *SMAD7* and *WNT5A*,[32,33] were investigated in TBX1-silenced PAd-derived cells. Although *SMAD7* transcripts were unaffected, *WNT5A* expression was reduced in TBX1-silenced PAd-derived cells (Figure 5C). Interestingly, most PAds with deregulated *TBX1* mRNA expression showed *WNT5A* mRNA

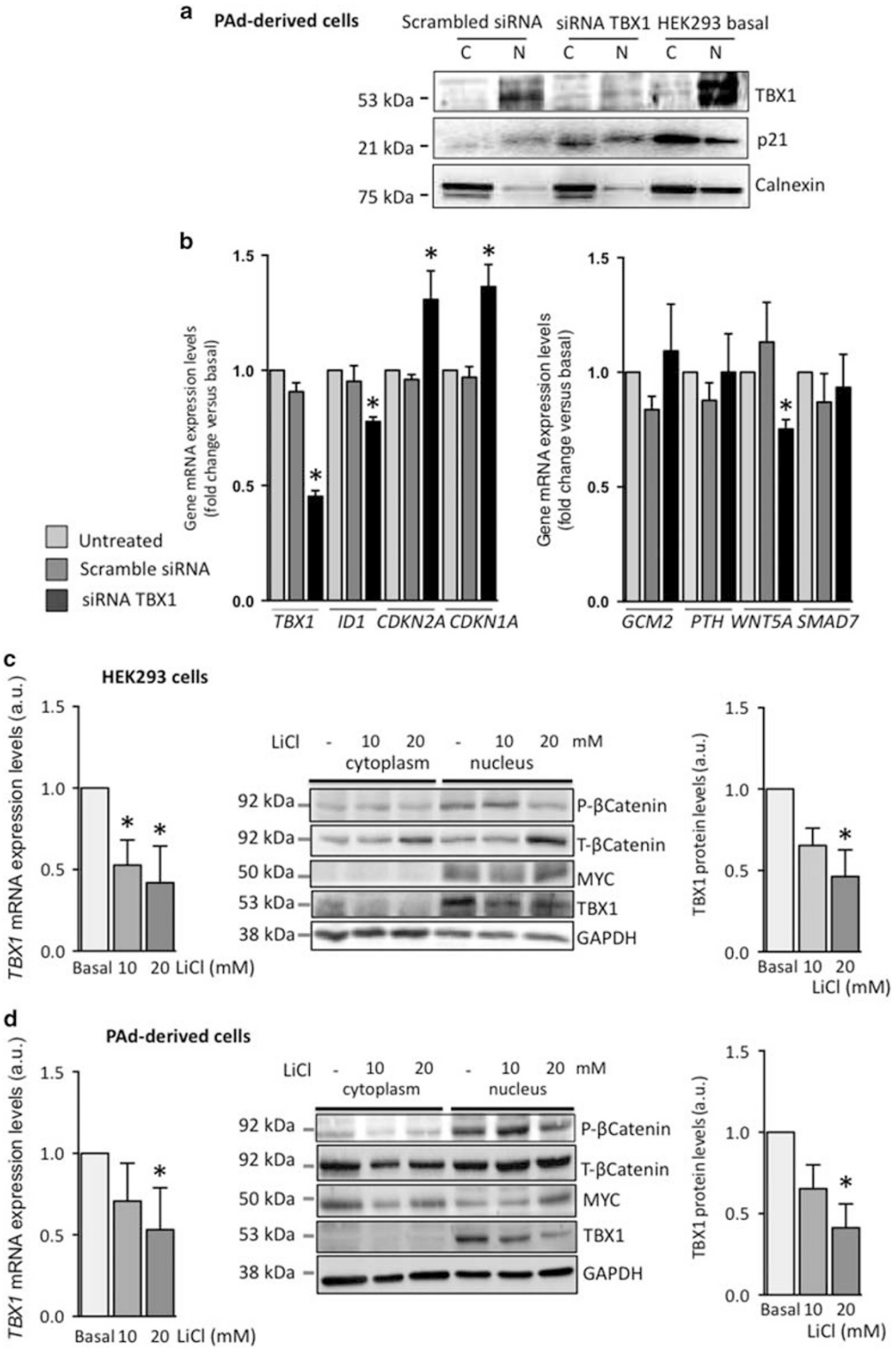


levels significantly reduced when compared with tumor samples with *TBX1* levels similar to those in PaNs ($1.36 \pm 0.69$ *vs* $4.67 \pm 1.15$; $P = 0.013$). Finally, in PAd-derived cells we tested the hypothesis that TBX1 might modulate the expression of the parathyroid-specific genes *GCM2* and *PTH*: no significant changes in *GCM2* and *PTH* transcript levels could be detected after 48 h of TBX1-silencing (Figure 5B).

### Regulation of TBX1 Gene Expression in PAd-Derived Cells

During embryonic development, the *TBX1* gene is transcriptionally regulated by Wnt/$\beta$-catenin pathway activation.[34,35] We tested the hypothesis that the Wnt/$\beta$-catenin pathway may regulate *TBX1* gene expression in PAd-derived cells. The effect of short-term activation of the Wnt/$\beta$-catenin pathway on *TBX1* mRNA expression levels was investigated *in vitro*. PAd-derived cells, and HEK293 cells used as controls, were treated for 8 h with increasing concentrations of lithium chloride (LiCl, 10–20 mM), an agent known to induce nuclear accumulation of $\beta$-catenin. Short-term LiCl treatment induced significant total $\beta$-catenin accumulation (and concomitant reduction in phosphorylated $\beta$-catenin) in the nuclear protein fractions of both HEK293 (Figure 5C) and PAd-derived cells (Figure 5D). The $\beta$-catenin nuclear accumulation was able to induce the expression of the known Wnt/$\beta$-catenin gene target MYC at nuclear levels, confirming that LiCl treatment determined Wnt pathway activation in both cell models (Figure 5C and D). Wnt/$\beta$-catenin pathway activation was associated with a reduction in *TBX1* mRNA levels in HEK293 cells and in five out of seven PAd-derived cell preparations and in nuclear TBX1 protein levels in both HEK293 and PAd-derived cells (Figure 5C and D).

## DISCUSSION

Investigation of the embryonic transcription factor TBX1 in human parathyroid tissues provided insights of potential interest. First, similar to other embryonic parathyroid transcription factors, namely *GCM2*, *GATA3*, and *HOX* genes, *TBX1* transcripts and proteins have been detected in a consistent subset of parathyroid cells of the adult normal glands. TBX1 immunoreactivity in FFPE sections and in total protein extracts from frozen PAd samples detected the 53 kDa product of the TBX1 isoform C, the more abundant isoform in human tissues.[36] TBX1 immunoreactivity has a nuclear and cytoplasmic localization confined to parathyroid epithelial cells, often coexpressing PTH; parathyroid endothelial cells lining vessels and stromal cells do not show specific immunoreactivity.

Tumor parathyroid cells retain the expression of *TBX1*, although it is variably deregulated in a subset of benign parathyroid tumors and in most parathyroid cancers, being associated with a reduced proportion of TBX1-expressing cells. In PAds, both *TBX1* transcripts' upregulation and downregulation were associated with loss of TBX1-expressing cells in a half of tumor samples, a condition resembling what demonstrated by genetic studies in patients with 22q11.2 microdeletion syndrome, where the same loss of function phenotype can be determined by both decreased and increased *TBX1* gene dosage.

Parathyroid carcinomas showed a particular signature, as reduced number of TBX1-expressing cells was associated with downregulation of *TBX1* transcripts and loss of parafibromin immunostaining. These data may suggest a regulatory relationship between parafibromin and TBX1.

The role of TBX1 in adult parathyroid cells is unknown. TBX1 is extensively involved in the embryonic development as shown by the wide spectrum of clinical alterations that affect patients with 22q11.2 microdeletion syndrome. During murine embryogenesis, Tbx1 is early expressed in the mesoderm core of the pharyngeal arches and in the pharyngeal endoderm.[12,37] *In situ* hybridization studies showed conserved stage specificity and localization of *TBX1* expression between mouse and human embryos. In early week six human embryos, *TBX1* expression was detected in the core mesenchyme of the first, second, and third pharyngeal arches and in the third pharyngeal pouches endoderm, the domain from which parathyroid cells originate.[38] TBX1 has to be expressed during embryogenesis to determine cell fate of endoderm-derived cells. Nonetheless, TBX1 expression during fetal development has not investigated so far. Here, immunohistochemistry analysis of human fetal tissues of 19–25 weeks of gestational age showed that TBX1 was expressed in both skeletal and smooth muscle cells and in the basal layer of tracheal epithelium. TBX1-expressing cells were detected in the fetal thyroid glands: location and expression of the podoplanin/D240 marker suggested that these cells lined lymphatic vessels, resembling what described in mice.[39] TBX1 is curiously absent in fetal parathyroid glands: it was faintly expressed in early fetal human

**Figure 5** Effects of TBX1 silencing in PAd-derived cells. (**a**) TBX1 was reduced by short interfering RNA (siRNA)-transient silencing in PAd-derived cells; the effect of TBX1 silencing on p21 protein expression levels is also shown. (**b**) Effects of TBX1 silencing on mRNA expression of potential target genes in PAd-derived cells; *$P > 0.05$ by ANOVA *vs* scramble siRNA for every analyzed gene. (**c**) Left panel: treatment for 8 h of HEK293 cells ($n = 3$) with increasing concentrations of LiCl (10 and 20 mM) induced a significant decrease in *TBX1* mRNA expression levels. Central panel: representative western blot analysis with specific antibodies of cytoplasmic and nuclear protein fractions from HEK293 cells treated with increasing concentrations of LiCl (10 and 20 mM) for 8 h showed that LiCl induced a nuclear accumulation of total $\beta$-catenin (T-$\beta$-catenin), a reduction of the inactive phosphorylated $\beta$-catenin (P-$\beta$-catenin) and a concomitant increase in the target gene MYC, consistent with the activation of the Wnt/$\beta$-catenin pathway. Concomitantly, nuclear TBX1 was reduced. Right panel: densitometric readings of the western blot data show LiCl-induced significant decrease in TBX1 protein levels; *$P < 0.05$ *vs* basal. (**d**) Left panel: treatment with LiCl of PAd-derived cells ($n = 7$) significantly reduced *TBX1* mRNA expression levels in five cell preparations. Central panel: western blot analysis of cytoplasmic and nuclear protein fractions from PAd-derived cells treated with LiCl for 8 h showed that LiCl induced a nuclear accumulation of total $\beta$-catenin (T-$\beta$-catenin), a reduction of the inactive phosphorylated $\beta$-catenin (P-$\beta$-catenin) and an increase in MYC, consistent with the activation of the Wnt/$\beta$-catenin pathway. Similar to what was observed in HEK293 cells, nuclear TBX1 was reduced. Right panel: densitometric readings of the western blot data show LiCl-induced significant decrease in TBX1 protein levels; *$P < 0.05$ *vs* basal.

parathyroid cells, expressing PTH, and undetectable in 25-week-gestational-age fetal parathyroid cells. TBX1 downregulation in fetal PTH-expressing parathyroid cells suggests that TBX1 is not required to sustain PTH expression in fetal parathyroid cells. PTH circulates at low concentrations in the fetal circulation. Fetal parathyroids are able to produce PTH, but PTH release is suppressed by calcium-sensing receptor activation secondary to the physiological fetal hypercalcemia.[40] Considering that fetal parathyroid cells are responsive to chronic hypocalcemia by developing hyperplasia, TBX1 silencing may be consistent with the quiescent status of progenitor cells, ready to enter cell cycle upon hypocalcemic stimuli. Resembling this 'fetal' hypothesis, we found in the present study that loss of TBX1-expressing cells in parathyroid tumors negatively correlated with hypercalcemia.

Besides the classical role of TBX1 in embryonic development, evidence about its involvement in cancers is accumulating. Members of the T-box family are involved in human tumorigenesis:[41] TBX2 and TBX3 are upregulated in several cancers, including melanoma, breast, lung, liver, pancreatic, ovarian, endometrial, and cervical cancers, whereas TBX5 and TBX18 are suppressed in the human colon cancer cell line RKO and in basal-like breast cancer, respectively. TBX18, which functions as an oncosuppressor, belongs to the TBX1 subfamily.[41] Moreover, the regulatory region of the *TBX1* gene has been found hypermethylated in human breast cancers.[42,43] The TBX1 downregulation detected in a subset of parathyroid tumors is in line with the report in breast cancer cells. Indeed, TBX1 silencing in HEK293 cells, endogenously expressing TBX1, determined an increase in the proportion of cells in the G0/G1 phase of cell cycle, associated with increased transcript levels of *CDKN1A*/p21 and *CDKN2A*/p16 and reduced *inhibitor of differentiation 1* (*ID1*) levels. Therefore, the cell cycle arrest is not consistent with a role as oncosuppressor of TBX1; however, it is similar to what detected in *Tbx1* knockout murine hair follicle stem cells.[44] *Tbx1*-deficient hair follicle stem cells remained quiescent longer than normal, but they eventually cycled. In this context, Tbx1 acts as a gatekeeper that governs the transition between stem cell quiescence and proliferation in hair follicle cells.[44] Although we were not able to investigate cell cycle in TBX1-silenced PAd-derived cells, TBX1 silencing in PAd-derived cells was associated with increased expression levels of *CDKN1A*/p21 and *CDKN2A*/p16 and reduced *ID1* levels, consistent with cell cycle arrest in G1.[45,46] Cell cycle arrest may explain the low cell proliferation rate characterizing clinically evident PAds.[47]

We looked for further potential effects of TBX1 silencing in PAd-derived cells: the specific parathyroid genes *GCM2* and *PTH* were not affected, resembling what detected in fetal parathyroid glands. Indeed, GCM2 is considered a downstream target of TBX1 during embryonic development[48] and high levels of GCM2 in parathyroid glands are required for maintenance of parathyroid cell differentiation and of high levels of calcium-sensing receptor expression.[49] However, these two embryonic transcription factors may act independently in tumor parathyroid cells.

Finally, parathyroid tumor cells retain the embryonic ability to regulate *TBX1* gene expression through Wnt/$\beta$-catenin activation; short-term treatment with lithium chloride induced $\beta$-catenin nuclear accumulation, increased the expression levels of the target gene MYC, and decreased *TBX1* transcript and protein levels. Besides, TBX1 silencing decreased the expression levels of *WNT5A*, which belongs to the non-canonical Wnt pathway and acts by inhibiting the canonical Wnt/$\beta$-catenin pathway.[50,51] We speculate that TBX1-deficient parathyroid tumor cells may experience a deregulated tuning of the Wnt/$\beta$-catenin pathway.

The present study provides unexplored insights in parathyroid tumors, although data here reported have some limits: (1) the effect of TBX1 silencing on cell cycle could not be investigated in parathyroid tumor cells; (2) timing is crucial in determining the effect of the molecules involved in cell cycle regulation, *CDKN1A*/p21, *CDKN2A*/p16, and ID1, although the present investigation was limited to 48 h after silencing, an early point in cell fate toward senescence, proliferation, or differentiation.

In conclusion, the embryonic transcription factor TBX1 is active and deregulated in parathyroid tumor cells, contributing to the definition of the heterogeneous parathyroid tumor cell phenotype. TBX1 deficiency may contribute to the low proliferation rate in parathyroid tumors in response to hypercalcemia and may be involved in WNT pathway deregulation.

Supplementary Information accompanies the paper on the Laboratory Investigation website (http://www.laboratoryinvestigation.org)

## ACKNOWLEDGMENTS

This research was supported by funds from Ricerca Corrente IRCCS Policlinico San Donato and IRCCS Istituto Ortopedico Galeazzi (L4080).

## DISCLOSURE/CONFLICT OF INTEREST

The authors declare no conflict of interest.

1. Günther T, Chen ZF, Kim J, *et al*. Genetic ablation of parathyroid glands reveals another source of parathyroid hormone. Nature 2000;406:199–203.
2. Manley NR, Capecchi MR. Hox group 3 paralogs regulate the development and migration of the thymus, thyroid, and parathyroid glands. Dev Biol 1998;195:1–15.
3. Betts G, Beckett E, Nonaka D. GATA3 shows differential immunohistochemical expression across thyroid and parathyroid lesions. Histopathology 2014;65:288–290.
4. Ordenez NG. Value of GATA3 immunostaining in the diagnosis of parathyroid tumors. Appl Immunohistochem Mol Morphol 2014;22:756–761.
5. Ding C, Buckingham B, Levine MA. Familial isolated hypoparathyroidism caused by a mutation in the gene for the transcription factor GCMB. J Clin Invest 2001;108:1215–1220.
6. Thomèe C, Schubert SW, Parma J, *et al*. GCMB mutation in familial isolated hypoparathyroidism wit residual secretion of parathyroid hormone. J Clin Endocrinol Metab 2005;90:2487–2492.

7. Mannstadt M, Bertrand G, Muresan M, *et al.* Dominat-negative GCMB mutations cause an autosomal dominant form of hypoparathyroidism. J Clin Endocrinol Metab 2008;93:3568–3576.
8. Correa P, Akerstrom G, Westin G. Underexpression of Gcm2, a master regulatory gene of parathyroid gland development, in adenomas of primary hyperparathyroidism. Clin Endocrinol 2002;57:501–505.
9. Kebebew E, Peng M, Wong MG, *et al.* GCMB gene, a master regulator of parathyroid gland development, expression, and regulation in hyperparathyroidism. Surgery 2004;136:1261–1266.
10. Shen HC, Rosen JE, Yang LM, *et al.* Parathyroid tumor development involves deregulation of homeobox genes. Endocr Relat Cancer 2008;15:267–275.
11. Vaira V, Elli F, Forno I, *et al.* The microRNA cluster C19MC is deregulated in parathyroid tumours. J Mol Endocrinol 2012;49:115–124.
12. Lindsay EA, Vitelli F, Su H, *et al.* Tbx1 haploinsufficiency in the DiGeorge syndrome causes aortic arch defects in mice. Nature 2001;410:97–101.
13. Xu H, Cerrato F, Baldini A. Timed mutation and cell-fate mapping reveal reiterated roles of Tbx1 during embryogenesis, and a crucial function during segmentation of the pharyngeal system via regulation of endoderm expansion. Development 2005;132:4387–4795.
14. Ryan AK, Goodship JA, Wilson DI, *et al.* Spectrum of clinical features associated with interstitial chromosome 22q11 deletions: a European collaborative study. J Med Genet 1997;34:798–804.
15. Passeri E, Frigerio M, De Filippis T, *et al.* Increased risk for non-autoimmune hypothyroidism in young patients with congenital heart defects. J Clin Endocrinol Metab 2011;96:E1115–E1119.
16. Arnold JS, Werling U, Braunstein EM, *et al.* Inactivation of Tbx1 in the pharyngeal endoderm results in 22q11DS malformations. Development 2006;133:977–987.
17. Baldini A, Fulcoli FG, Illingworth E. TBX1: transcriptional and developmental functions. Curr Top Dev Biol 2017;122:223–243.
18. Palena C, Polev DE, Tsang KY, *et al.* The human T-box mesodermal transcription factor Brachyury is a candidate target for T-cell-mediated cancer immunotherapy. Clin Cancer Res 2007;13:247–248.
19. Rodriguez M, Aladowicz E, Lanfrancone L, Goding CR. Tbx3 represses E-cadherin expression and enhances melanoma invasiveness. Cancer Res 2008;168:7872–7881.
20. Li J, Ballim D, Rodriguez M, *et al.* The anti-proliferative function of the TGF-β1 signaling pathway involves the repression of the oncogenic TBX2 by its homologue TBX3. J Biol Chem 2014;289:35633–35643.
21. Trempus CS, Wei S-J, Humble MM, *et al.* A novel role for the T-box transcription factor *Tbx1* as a negative regulator of tumor cell growth in mice. Mol Carcinog 2011;50:981–991.
22. Larsimont J-C, Youssef KK, Sanchez-Danes A, *et al.* Sox9 controls self-renewal of oncogene targeted cells and links tumor initiation and invasion. Cell Stem Cell 2015;17:60–73.
23. Corbetta S, Bulfamante G, Cortelazzi D, *et al.* Adiponectin expression in human fetal tissues during mid- and late gestation. J Clin Endocrinol Metab 2005;90:2397–2402.
24. Bondeson L, Grimelius L, DeLellis RA, *et al.* Parathyroid carcinoma. In: DeLellis RA, Lloyd RV, Heitz PU & Eng C (eds). Pathology and Genetics. Tumors of Endocrine Organs. WHO Classification of Tumors. IARC Press: Lyon, France, 2004, pp 128–132.
25. Corbetta S, Vaira V, Guarnieri V, *et al.* Differential expression of microRNAs in human parathyroid carcinomas compared with normal parathyroid tissue. Endocr Relat Cancer 2010;17:135–146.
26. Cetani F, Ambrogini E, Viacava P, *et al.* Should parafibromin staining replace HRPT2 gene analysis as an additional tool for histologic diagnosis of parathyroid carcinoma? Eur J Endocrinol 2007;156:547–554.
27. Guarnieri V, Battista C, Muscarella LA, *et al.* CDC73 mutations and parafibromin immunohistochemistry in parathyroid tumors: clinical correlations in a single-centre patient cohort. Cell Oncol 2012;35:411–422.
28. Cetani F, Banti C, Pardi E, *et al.* CDC73 mutational status and loss of parafibromin in the outcome of parathyroid cancer. Endocr Connect 2013;2:189–195.
29. Forno I, Ferrero S, Russo MV, *et al.* Deregulation of Mir-34b/Sox2 predicts prostate cancer progression. PLoS ONE 2015;10:e0130060.
30. Cetani F, Pardi E, Borsari S, *et al.* Genetic analyses of the HRPT2 gene in primary hyperparathyroidism: germline and somatic mutations in familial and sporadic parathyroid tumors. J Endocrinol Invest 2004;89:5583–5591.
31. Guarnieri V, Scillitani A, Muscarella LA, *et al.* Diagnosis of parathyroid tumors in familial isolated hyperparathyroidism with HRPT2 mutation: implications for cancer surveillance. J Clin Endocrinol Metab 2006;91:2827–2832.
32. Papangeli I, Scambler PJ. Tbx1 genetically interacts with the transforming growth factor-β/bone morphogenetic protein inhibitor Smad7 during great vessel remodeling. Circ Res 2013;112:90–102.
33. Chen L, Fulcoli FG, Ferrentino R, *et al.* Transcriptional control in cardiac progenitors: Tbx1 interacts with the BAF chromatin remodeling complex and regulates Wnt5a. PLoS Genet 2012;8:e1002571.
34. Huh SH, Ornitz DM. Beta-catenin deficiency causes DiGeorge syndrome-like phenotypes through regulation of Tbx1. Development 2010;137:1137–1147.
35. Freyer L, Morrow BE. Canonical Wnt signaling modulates Tbx1, Eya1, and Six1 expression, restricting neurogenesis in the otic vescicle. Dev Dyn 2010;239:1708–1722.
36. Gong W, Gottlieb S, Collins J, *et al.* Mutation analysis of *TBX1* in non-deleted patients with features of DGS/VCFS or isolated cardiovascular defects. J Med Genet 2001;38:e45.
37. Garg V, Yamagishi C, Hu T, *et al.* Tbx1, a DiGeorge syndrome candidate gene, is regulated by sonic hedgehog during pharyngeal arch development. Dev Biol 2001;235:62–73.
38. Farley AM, Morris LX, Vroegindeweij E, *et al.* Dynamics of thymus organogenesis and colonization in early human development. Development 2013;140:2015–2026.
39. Chen L, Mupo A, Huynh T, *et al.* Tbx1 regulates Vegfr3 and is required for lymphatic vessel development. J Cell Biol 2010;189:417–424.
40. Kovacs CS. Bone development and mineral homeostasis in the fetus and neonate: roles of the calciotropic and phosphotropic hormones. Physiol Rev 2014;94:1143–1218.
41. Takashima Y, Suzuki A. Regulation of organogenesis and stem cell properties by T-box transcription factors. Cell Mol Life Sci 2013;70:3929–3945.
42. Rønneberg JA, Fleischer T, Solvang HK, *et al.* Methylation profiling with a panel of cancer related genes: association with estrogen receptor, TP53 mutation status and expression subtypes in sporadic breast cancer. Mol Oncol 2011;5:61–76.
43. Conway K, Edmiston SN, May R, *et al.* DNA methylation profiling in the Carolina Breast Study defines cancer subclasses differing in clinico-pathologic characteristics and survival. Breast Cancer Res 2014;16:450.
44. Chen T, Heller E, Beronja S, *et al.* An RNA interference screen uncovers a new molecule in stem cell self-renewal and long-term regeneration. Nature 2012;485:104–110.
45. Mern DS, Hoppe-Seyler K, Hoppe-Seyler F, *et al.* Targeting Id1 and Id3 by a specific peptide aptamer induces E-box promoter activity, cell cycle arrest, and apoptosis in breast cancer cells. Breast Cancer Res Treat 2010;124:623–633.
46. Imai H, Kato S, Sakamoto Y, *et al.* High throughput RNAi screening identifies ID1 as a synthethic sick/lethal gene interacting with the common TP53 mutation R175H. Oncol Rep 2014;31:1043–1050.
47. Parfitt AM, Wang Q, Palnitkar S. Rates of cell prolifertion in adenomatous, suppressed, and normal parathyroid tissue: implications for pathogenesis. J Clin Endocrinol Metab 1998;83:863–869.
48. Ivins S, Lammerts Van Beuren K, Roberts C, *et al.* Microarray analysis detects differentially expressed genes in the pharyngeal region of mice lacking Tbx1. Dev Biol 2005;285:554–569.
49. Mizobuchi M, Ritter CS, Krits I, *et al.* Calcium-sensing receptor expression is regulated by glial cells missing-2 in human parathyroid cells. J Bone Miner Res 2009;24:1173–1179.
50. Yuan Y, Niu CC, Deng G, *et al.* The Wnt5a/Ror2 noncanonical pathway inhibits canonical Wnt signaling in K562 cells. Int J Mol Med 2011;27:63–69.
51. Park HW, Kim YC, Yu B, *et al.* Alternative Wnt signaling activates YAP/TAZ. Cell 2015;162:780–794.